Low-frequency radiation of relativistic particles moving along the arc of a circle

B. M. Bolotovskiĭ and A. V. Serov

Lebedev Physics Institute, Russian Academy of Sciences

Spectral-angular distribution of low-frequency radiation of electrons moving along the arc of a circle has been measured. The experiments have shown that radiation intensity distributions differ from synchrotron ones even for particle deviation angles much larger than γ^{-1} in the turning magnet field. An analytic expression for the spectral-angular distribution of low-frequency radiation has been found and shown to be in agreement with the measurements.

INTRODUCTION

The radiation of relativistic charged particles in inhomogeneous fields has been investigated in detail (see Refs. 1 and 2 and the citations therein) basically for two reasons. First, this radiation forms a background in undulator-radiation sources, based on electron synchrotrons and storage rings.[3,4] Second, it is this very radiation that allows diagnostics of proton synchrotron beams by optical methods.[5,6] In both cases only the high-frequency spectral region, where the radiation power is the greatest, has been studied. In the low-frequency region the radiation power is low and decreases as $\omega^{1/3}$. This is probably why the low-frequency radiation has not yet been analyzed. In the low-frequency region, however, the wavelength can become of the order of the bunch size. Electrons are emitted coherently, and the radiation power increases by a factor of N in comparison with the case of incoherent radiation (N is the number of particles in a bunch). This increase can be larger than the radiation-power drop in the low-frequency region. Generation of low-frequency radiation of particles moving along the arc of a circle has been considered in Ref. 7. However only the generation at a very low (zero) frequency has been studied (i.e., the case $\omega \to 0$ has been considered), and the results do not allow to calculate the spectral-angular distribution of low-frequency radiation.

In the present work the spectral-angular and polarization characteristics of low-frequency particle radiation have been measured. It has turned out that the results can be explained by invoking the Huygens principle, according to which the radiation from a finite section of an orbit is the result of interference of the waves emitted by a particle at each point of its path. Therefore, for example, if the charge radiation from a finite section of the path is observed at a distant point (when the distance to the observer is large in comparison with the orbit size), the radiation is formed as in Fraunhofer diffraction. If, however, the distance between the observation point and the orbit is comparable to the orbit length, there is a close analogy with Fresnel diffraction. As the measurements have shown, the distributions have some features which, apart from their theoretical significance, may turn out to be important practically.

1. EXPERIMENTAL PROCEDURE

The experimental setup is shown in Fig. 1. Relativistic electrons were emitted from a microtron. The accelerated current comprised a sequence of electron bunches of length 10 mm each following each other at a distance 100 mm. The electron energy E was 7.2 MeV and the current I was 40 mA in a pulse of length 4 μs. The particles were transported along a path containing correctors and lenses and were extracted from the microtron vacuum volume into the atmosphere through a copper foil of width 100 μm at the path flange *1*. The beam passed next through a turning magnet *2* and was absorbed in a Faraday cylinder *3*. The turning magnet of width 80 mm created a field of amplitude $H = 1000$ Oe in which the particles were deflected by an angle $\alpha = 20°$. Note that this angle is much larger than the characteristic angle $v^{-1} = 3.5°$, where $\gamma = E/mc^2$, so that the turning magnet cannot be considered "short".[5–7] The orbit section from which the electromagnetic radiation was collected was situated in the air between the foil through which the beam passed and the Faraday cylinder. This part of the orbit is shown in Fig. 1 by a dashed line. The radiation intensity was measured by a receiver *4* containing a silicon point diode D-407 or D-402 and an amplifier. The diode D-407 has the greatest sensitivity at wavelengths 5 to 7 mm, and the diode D-402 at wavelengths 10–12 mm. These wavelengths lie in the low frequency region of radiation spectrum, since the critical wavelength near which the maximum of the radiation spectral distribution is situated is equal, in our case, to $\lambda = 4\pi r_0/3\gamma^3 = 0.3$ mm, where r_0 is the orbit radius. The diode is constructed in such a way that it detects only that part of radiation which has a definite polarization with respect to the diode receiving window. This gave us the possibility to detect the σ- and π-components of the radiation polarization by rotating the diode about its axis. The radiation receivers could be remotely moved in the horizontal plane perpendicular to the path axis. This allowed us to measure the horizontal distribution of the intensity of the σ and π components of radiation polarization at various wavelengths. Variation of the position of the radiation receiver changed the angle φ between the tangent to the beam orbit in the middle of the turning magnet (the y-axis in Fig. 1) and the line connecting the magnet and the receiver.
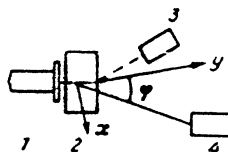

FIG. 1. Diagram of the experimental setup.

2. DISCUSSION

Typical horizontal-angular distributions of the measured radiation intensity are shown in Fig. 2. It is seen that if the observation angle changes, the σ component of the radiation intensity grows from nearly zero at small angles to a maximum at a certain angle that depends on the wave-length of the detected radiation. Note that such dependences are not at all typical of relativistic particle radiation in a magnetic field. It follows from the theory that the radiation is directed along the tangent to the orbit and is concentrated in a narrow beam of angular width γ^{-1}. Therefore only the radiation generated by an electron over a short part of its trajectory, of length r_0/γ (Ref. 1), is detected at the observation point. Accordingly, when particles are turned in magnetic field through an angle larger than γ^{-1} the greatest radiation intensity must be observed at angles $\varphi \approx 0$. In the experiments, however, the maximum of the σ-component of radiation is observed for angles not only not equal to zero but much larger than the angles γ^{-1}. (In our case $\gamma^{-1} \approx 3.5°$ and the radiation maximum corresponded to $\varphi \approx 12°$ at $\lambda \approx 7$ mm and to $\varphi \approx 18°$ at $\lambda \approx 12$ mm.)

It is known[8] that if a charged particle moves according to a law $\mathbf{r}(t)$, the radiation field at a frequency ω can be expressed in terms of the Fourier component $\mathbf{A}_\omega(\mathbf{r})$ of the vector potential:

$$\mathbf{A}_\omega(\mathbf{r}) = \frac{q}{c}\int_{-\infty}^{\infty} \frac{\mathbf{v}(t)}{|\mathbf{r}-\mathbf{r}(t)|}\exp\left[i\omega\left(t - \frac{|\mathbf{r}-\mathbf{r}(t)|}{c}\right)\right]dt.$$

(1)

Here $\mathbf{v}(r) = d\mathbf{r}(t)/dt$ is the charge velocity at the time t, $\mathbf{r}$ is the radius-vector of the observation point, and q is the charge. If the observation point is far enough from the charge trajectory, so that the distance between the observation point and the trajectory is large in comparison with the orbit size, Eq. (1) takes the simpler form

I_ϕ, rel. units

I_π, rel. units

FIG. 2. Experimental horizontal-angular distribution of intensity of the σ (a)- and π (b)-components of radiation polarization: a) $\theta = 0$, $\lambda = 12$ mm (1) and 7 mm (2; b) $\theta = 0.2$, $\lambda = 12$ mm.

$$\mathbf{A}_\omega(\mathbf{r}) = \frac{\exp(ikR)}{cR}\int_{-\infty}^{\infty} q\mathbf{v}(t)\exp\{i[\omega t - \mathbf{kr}(t)]\}\,dt,$$

(2)

where R is the distance between the orbit and the observation point, $\mathbf{k}$ is the wave vector of the emitted wave ($k = \omega/c$, and the vector $\mathbf{k}$ points from the orbit to the observation point). Let the particle move along a trajectory in the xy-plane (see Ref. 8, Sec. 74, Fig. 16, where the same geometry is adopted). The trajectory is a part of a circle of radius r_0 between the azimuths $\varphi = \varphi_1$ and $\varphi = \varphi_2$. The observation point lies on the y-axis far enough from the orbit center, i.e., $k_x = 0$. From Eq. (2) we can get the expressions for the σ- and π-components of the radiation field vector-potential:

$$A_{\omega,\sigma} = v\frac{\exp(ikR)}{cR}\int_{\varphi_1}^{\varphi_2} q\sin\varphi\exp\left[in\left(\varphi - \frac{v}{c}\cos\theta\sin\varphi\right)\right]d\varphi,$$

(3)

$$A_{\omega,\pi} = v\theta\frac{\exp(ikR)}{cR}\int_{\varphi_1}^{\varphi_2} q\cos\varphi\exp\left[in\left(\varphi - \frac{v}{c}\cos\theta\sin\varphi\right)\right]d\varphi,$$

where $\varphi = \omega_0 t$, ω_0 is the frequency of electron rotation along the circular orbit, $\omega_0 = v/r_0$, θ is the angle between the xy-plane and the radiation direction, and $n = \omega/\omega_0$. In the case of a uniform rotation along the circle, the integration is performed over the full circle, from $\varphi = 0$ to $\varphi = 2\pi$. In the meaurements described above the difference $\varphi_1 - \varphi_2$ remained constant and comprised 20°. In the experiment, when the detector is moved, its position with respect to the emitting section of the orbit changes. In integrals (3) we allowed for this by varying the position of the emitting region and assuming that the observation point is fixed. When the observation angle changed, the arc of the circle contained between the angles $\varphi = \varphi_1$ and $\varphi = \varphi_2$ moved along the circle. The observation angle changed from $\varphi \approx 0°$ to $\varphi \approx 30°$. In Fig. 1 the observation angle $\varphi = 0$ corresponds to the direction of the y-axis and can be varied only in one direction, owing to the setup geometry.

As is known,[1] synchrotron radiation has the greatest intensity near a wavelength $\lambda = 4\pi a/3\gamma^3$ called critical. For such wavelengths the radiation is collected from a small orbit portion of length r_0/γ. If this ratio is smaller than the arc length $r_0(\varphi_1 - \varphi_2)$, the integration limits in (3) can be extended to the full circle. Then the motion along a finite arc gives the same spectrum as the ordinary synchrotron radiation. If, however, radiation at sufficiently large wavelengths is considered, as in our case, the results depend substantially on the size of the arc along which an electron moves, and on its position on the circle. To find this dependence, we have performed numerical calculations using Eq. (3). The results are shown by a solid line in Fig. 3. It is seen that they are in qualitative agreement with the measurements. The intensity modulations seen on the experimental curves are caused by higher radiation harmonics ($\lambda = 1-2$ mm) which can also be detected by the diodes.

The spectral-angular distribution of low-frequency radiation, which arises when a particle moves along a finite arc, can be described analytically with the help of approximate formulas which are found from (3) under the assumption that in the integration limits the phase variation in the
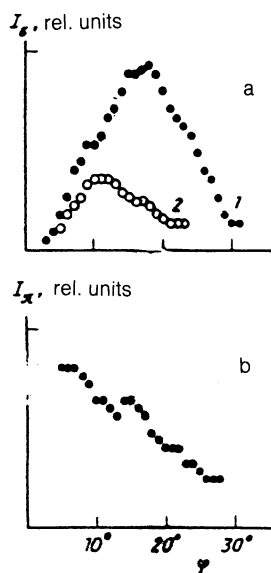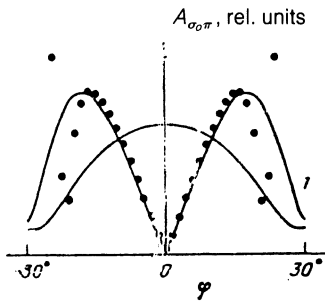
816   Sov. Phys. JETP 75 (5), November 1992

B. M. Bolotovskiĭ and A. V. Serov   816

$A_{\sigma\sigma\pi}$, rel. units

-30°   0   30°
φ

FIG. 3. Angular distributions of the components A_σ (1,●) and A_π (2) of the vector-potential: curves 1 and 2 correspond to numerical integration of Eq. (3), and the closed circles to calculations by the formula (4); $\lambda = 12$ mm, $\varphi_1 - \varphi_2 = 20°$, $\theta = 0(1)$, and $0.2(2)$.

exponent is small in comparison with unity. This assumption is valid, if the radiation harmonic number n and the angular size $\Delta\varphi$ of the carc, along which the charge moves, satisfy the condition $\Delta\varphi \leqslant (6/n)^{1/3}$. In this case the exponential in the integrand in (3) can be expanded in the powers of its argument, with account taken of powers not higher than the fourth. Thus, the following expressions are derived from (3):

$$A_{\omega,\sigma,\pi}=A_{\omega,\sigma,\pi}(\varphi_2)-A_{\omega,\sigma,\pi}(\varphi_1), \qquad (4)$$

where

$$A_{\omega,\sigma}(\varphi_{1,2}) = qv\,\frac{\exp(ikR)}{cR}\left[\sum_1^6 a_i\varphi_{1,2}^{2i+1} + i\sum_1^8 b_j\varphi_{1,2}^{2j}\right],$$

$a_1=d/3$, $a_2=(n-d^3-d)/5\cdot6$, $a_3=(d^3-n-3nd)/7\cdot36$,

$a_4=(d^2n-dn^2)/9\cdot72$, $a^5=(dn^2-n^3/18)/11\cdot72$, $a_6=n^3/13\cdot6^3$,

$b_1=1/2$, $b_2=(-3d^2-1)/4\cdot6$, $b_3=(36d^4-dn+3d^2)/6\cdot36$,

$b_4=(6dn-n^2+48d^3n-12d^4)/8\cdot72$,

$b_5=(n^2/12+6d^2n^2+4d^3n)/10\cdot36$,

$b_6=(2dn^3/3-3d^2n^2/2)/12\cdot36$, $b_7=(n^4-4dn^3)/14\cdot6^3$,

$b_8=n^4/16\cdot6^5$,

$d=n(1/\gamma^2+\theta^2)/2$,

$$A_{\omega,\pi}(\varphi_{1,2}) =\theta qv\,\frac{\exp(ikR)}{cR}\left[\sum_1^5 c_i\varphi_{1,2}^{2i-1} + i\sum_1^6 f_j\varphi_{1,2}^{2j}\right],$$

$c_1=1$, $c_2=(-d^2-1)/6$, $c_3=(d^2-2dn/3)/20$,

$c_4=(nd-n^2/6)/7\cdot12$,

$c_5=n^2/6^4$, $f_1=d/2$, $f_2=(n-3d-d^3)/24$,

$f_3=(-d^2n+d^3-d)/72$,

$f_4=(d^2n-dn^2/3)/24\cdot8$, $f_5=(dn^2/4-n^3/36)/10\cdot36$,

$f_6=n^3/4\cdot6^5$.

The results found in this approximation are shown by points in Fig. 3. As is seen, they agree with the results of exact

numerical calculations in the range of observation angles, where the assumption that the phase in the argument of the exponential is small is valid.

CONCLUSION

By now we know well some relatively simple cases of moving-particle radiation, such as transition radiation, synchrotron radiation, undulator radiation, diffraction radiation, the Cerenkov–Vavilov radiation, etc. Each of these types of radiation arises only when certain physical conditions are satisfied. For example, the Cerenkov radiation arises when a charged particle moves uniformly and in a straight line in an infinite refracting medium with velocity higher than the phase velocity of light in this medium. Transition radiation arises when a charged particle, moving uniformly and in a straight line, crosses a plane interface of two semi-infinite media. Synchrotron radiation arises when a charge moves along a sufficiently long circular orbit.

In practice, however the conditions determining the type of radiation are far from being met. In particular, the charge motion is far from uniform and straight-line, the real medium is always finite, often inhomogeneous; all this should be taken into account when we compare theory with experiment. When a charge enters a Cerenkov counter or leaves an emitter, bursts of transition radiation arise, so that it is necessary to allow for the interference of this radiation with the Cerenkov radiation generated in the emitter. The radiation of a charge moving along a finite arc of a circle can differ from the synchrotron one, and the differences may vary from one spectral region to another. In particular, at frequencies close to the critical one and at higher frequencies the synchrotron radiation is formed on orbit sections of angular size γ^{-1}, i.e., even when a charge moves along a small arc of angular size γ^{-1} the synchrotron radiation is ordinary with respect to both spectrum and angular distribution. Bear in mind that here we speak of radiation harmonics with a sufficiently large number $n = \omega/\omega_0 \approx \gamma^3$. If the number of the harmonic is not so large (in the experiment $n \approx 30$, whereas the critical-harmonic number is of order 10^3), the radiation formed over a finite arc differs greatly in its spectral-angular distribution from synchrotron radiation. Note, however, that Eq. (3) is universal and describes radiation in all cases.

[1] I. M. Ternov and V. V. Mikhailin, *Synchrotron Radiation*, Energoatomizdat, Moscow, 1986.
[2] M. M. Nikitin and V. Ya. Epp, *Undulator Radiation*, Energoatomizdat, Moscow, 1988.
[3] M. M. Nikitin, A. F. Medvedev, N. B. Moiseev et al., Zh. Eksp. Teor. Fiz. 79, 763 (1980) [Sov. Phys. JETP 52, 388 (1980)].
[4] Yu. A. Bashmakov, Zh. Tekh. Fiz. 56, 515 (1986) [Sov. Phys. Tech. Phys. 31, 310 (1986)].
[5] R. Coisson, Phys. Rev. A 20, 524 (1979).
[6] N. V. Smolyakov, Zh. Eksp. Teor. Fiz. 56, 1262 (1979) [Sov. Phys. Tech. Phys. 31, 714 (1986)].
[7] V. G. Bagrov, I. M. Ternov, and N. I. Fedosov, Zh. Eksp. Teor. Fiz. 82, 1442 (1982) [Sov. Phys. JETP 55, 835 (1982)].
[8] L. D. Landau and E. M. Lifshitz, *The Classical Theory of the Fields*, Pergamon, 1975.

Translated by E. Khmelnitski